NOAA Technical Report NESDIS 5

A Statistical Technique for Forecasting Severe Weather From Vertical Soundings by Satellite and Radiosonde

Washington, D.C.
June 1983

U.S. DEPARTMENT OF COMMERCE
National Oceanic and Atmospheric Administration
National Environmental Satellite, Data, and Information Service

NOAA TECHNICAL REPORTS

National Environmental Satellite, Data, and Information Service

The National Environmental Satellite, Data, and Information Service (NESDIS) manages the Nation's civil operational Earth-observing satellite systems, as well as global national data bases for meteorology, oceanography, geophysics, and solar-terrestrial sciences. From these sources, it develops and disseminates environmental data and information products critical to the protection of life and property, national defense, the national economy, energy development and distribution, global food supplies, and the development of natural resources.

Publication in the NOAA Technical Report series does not preclude later publication in scientific journals in expanded or modified form. The NESDIS series of NOAA Technical Reports is a continuation of the former NESS and EDIS series of NOAA Technical Reports and the NESC and EDS series of Environmental Science Services Administration (ESSA) Technical Reports.

These reports are available from the National Technical Information Service (NTIS), U.S. Department of Commerce, Sills Bldg., 5285 Port Royal Road, Springfield, VA 22161. Prices on request for paper copies or microfiche.

A more complete listing of these reports, by title and NTIS accession number, is available from the Assessment and Information Services Center, National Oceanic and Atmospheric Administration, Code E/AI13, Page Bldg. 2, 3300 Whitehaven Street, N.W., Washington, DC 20235. A partial listing of more recent reports appears below:

NESS Series

NESS 89 A Statistical Approach to Rainfall Estimation Using Satellite and Conventional Data. Linwood F. Whitney, Jr. April 1982. (PB82 215435)

NESS 90 Total Precipitable Water and Rainfall Determinations From the SEASAT Scanning Multichannel Microwave Radiometer (SMMR). John C. Alishouse, May 1982. (PB83 138263)

NESS 91 Numerical Smoothing and Differentiation by Finite Differences. Henry E. Fleming and Lawrence J. Crone, May 1982. (PB82-258385)

NESS 92 Satellite Infrared Observations of Oceanic Long Waves in the Eastern Equatorial Pacific 1975 to 1981. Richard Legeckis, November 1982. (PB83 161133)

NESS 93 A Method for Improving the Estimation of Conditional Instability from Satellite Retrievals. W.E. Togstad, J.M. Lewis, and H.M. Woolf, November 1982. (PB83 169938)

EDIS Series

EDS 29 GATE Convection Subprogram Data Center: Final Report on Rawinsonde Data Validation. Robert W. Reeves, March 1978. (PB-281-861)

EDS 30 Gamma Distribution Bias and Confidence Limits. Harold L. Crutcher and Raymond L. Joiner, September 1978. (PB-289-721)

EDIS 31 Calibration and Intercomparison of the GATE C-Band Radars. M. Hudlow, R. Arkell, V. Patterson, P. Pytlowany, F. Richards, and S. Geotis (MIT), November 1979. (PB81 120305)

EDIS 32 Distribution of Radiosonde Errors. Harold L. Crutcher, May 1979. (PB-297-383)

EDIS 33 Accurate Least-Squares Techniques Using the Orthogonal Function Approach. Jerry Sullivan, March 1980. (PB80 223241)

EDIS 34 An Application of Stochastic Forecasting to Monthly Averaged 700 mb Heights. Albert Koscielny, June 1982. (PB82 244625)

NESDIS Series

NESDIS 1 Satellite Observations on Variations in Southern Hemisphere Snow Cover. Kenneth F. Dewey and Richard Heim, Jr., June 1983. (PB83 252908)

NESDIS 2 NODC 1 An Environmental Guide to Ocean Thermal Energy Conversion (OTEC) Operations in the Gulf of Mexico. National Oceanographic Data Center (DOC/NOAA Interagency Agreement Number EX-76-A-29-1041), June 1983.

NESDIS 3 Determination of the Planetary Radiation Budget From TIROS-N Satellites. Arnold Gruber, Irwin Ruff, and Charles Earnest, August 1983.

NESDIS 4 Some Applications of Satellite Radiation Observations to Climate Studies. T. S. Chen, George Ohring, and Haim Ganot, September 1983.

NOAA Technical Report NESDIS 5

A Statistical Technique for Forecasting Severe Weather From Vertical Soundings by Satellite and Radiosonde

David L. Keller
and William L. Smith

Washington, D.C.
June 1983

U.S. DEPARTMENT OF COMMERCE
Malcolm Baldrige, Secretary

National Oceanic and Atmospheric Administration
John V. Byrne, Administrator

National Environmental Satellite, Data, and Information Service
John H. McElroy, Acting Assistant Administrator

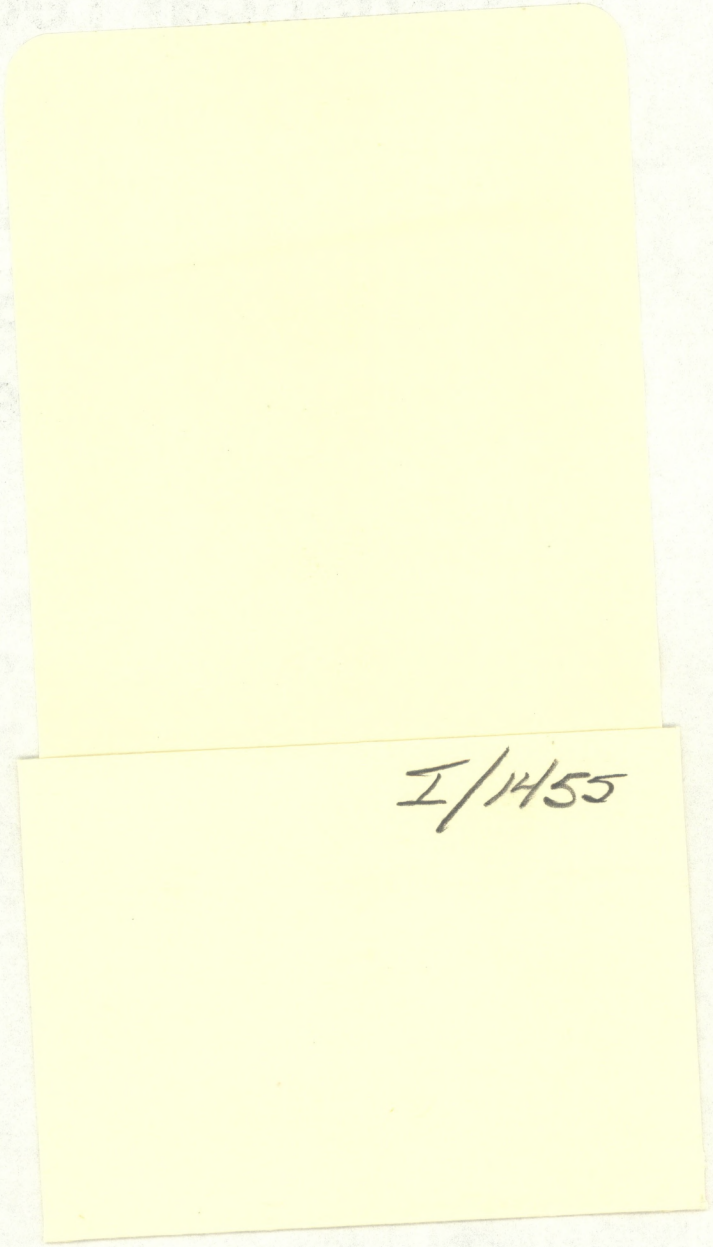
I/1455

CONTENTS

FIGURES

Appendix

A STATISTICAL TECHNIQUE FOR FORECASTING SEVERE WEATHER FROM VERTICAL SOUNDINGS BY SATELLITE AND RADIOSONDE

David L. Keller[1] and William L. Smith[2]
[1]Space Science and Engineering Center, Univ. of Wisconsin, Madison, WI, 53706
[2]NOAA/NESDIS Development Laboratory, 1225 W. Dayton St., Madison, WI, 53706

Abstract

An objective non-linear forecast technique is developed. Its value for severe weather forecasting using high spatial density NOAA-6 polar orbiting satellite soundings is compared with the forecasting skill achieved with radiosonde data. Gridpoint analyses of tropospheric temperatures, dewpoints, and winds are used to calculate stability and dynamic predictors. A non-linear "graphical" regression technique is used to evaluate the predictors individually and in combination, with the data being divided into 21 dependent and ten independent days (or cases) obtained during the 1981 severe weather season. Forecasts of severe weather on the independent days using the higher resolution satellite data resulted in "threat" scores which are equal to and slightly higher than the threat scores of forecasts made from radiosonde data. Using the NOAA-6 polar orbiting satellite derived severe weather probability equations, a case study is done using geosynchronous satellite VAS sounding data, demonstrating its capability of monitoring severe weather potential throughout the day.

1. Introduction

Severe weather events are small scale features, usually being isolated and widely scattered in space and time. Early in the day, forecasters must subjectively infer afternoon and evening mesoscale severe weather events from the synoptic scale features and forcing described by the radiosonde and surface observation network. As short lived mesoscale events, predictions of severe weather for periods exceeding a few hours are limited to outlining relatively large areas where severe weather might occur.

Operationally, an "outlook" for severe weather is issued at approximately 1500 GMT. The outlook is based mainly upon stability and dynamic parameters derived from the 1200 GMT radiosonde data, and numerical model forecasts of these parameters. Commonly used examples of these are the Showalter and lifted indices, the "K" and total totals indices, and the "SWEAT" indices. The first four of these are thermally based stability indices. The SWEAT (Severe WEAther Threat) index includes the 850 and 500 mb wind speeds and the angle between them (a measure of the 850-500 mb vertical wind shear), three dynamic factors commonly used in severe weather forecasting.

For severe weather applications, three limitations of radiosonde data become apparent. "Aliasing," the use of a single "point" measurement to represent a large area, becomes a significant problem in pinpointing severe weather. Secondly, the timeliness of the data is not optimal, as surface heating which affects convection is not strongly felt until after 1200 GMT. Thirdly, the relatively wide spacing of radiosonde data limits the ability of objective analyses in pinpointing the locations and magnitudes of strong gradients. It is often in the areas possessing strong moisture and thermal gradients that severe weather is most likely to occur.

The NOAA-6 polar orbiting satellite with its infrared and microwave radiometers allows quantitative measurements to be made of the troposphere at a much higher horizontal resolution. Vertical profiles of temperatures and dewpoints are calculated from these radiometric measurements (Smith et al., 1979). From the temperature and moisture data, pressure height fields are calculated using the hypsometric equation, from which gradient winds are calculated. As such, the satellite soundings provide an upper air data set which can be utilized in much the same manner as conventional radiosonde data.

NOAA-6 soundings are commonly produced with an average horizontal density five times that of the radiosonde data. This density should substantially reduce aliasing, as well as allow magnitudes of thermal and moisture gradients to be specified more precisely. In addition, the locations of the maximum values of scalar quantities should be positioned with greater accuracy. In particular, Blechman (1981) showed that the jet stream, which is a function of the thermal gradient in the troposphere, can be located very accurately using satellite soundings.

The moisture field also benefits from the higher data density. Hayden et al. (1981) demonstrated that strong gradients of the moisture field are accurately portrayed by satellite soundings.

A characteristic of the satellite temperature and moisture soundings is their low vertical resolution. The radiosonde often shows a great amount of

detail, especially in the vertical dewpoint profile. Often in situations favorable to severe weather, the moisture at 1200 GMT will be confined entirely under the 850 mb level, the level at which many of the stability indices use the dewpoint temperature. In these cases, the radiosonde will yield indices of stability that are relatively low. The satellite's tendency to average this moisture in the vertical direction can result in a dewpoint that is more representative of the moisture available for severe weather.

The purpose of this study is to develop an objective forecast technique and to use it to evaluate the utility of satellite soundings in the forecasting of severe weather. The objective technique is used to compare the forecast skill using satellite data to that using radiosonde data. A dependent data set is used to relate severe weather predictors derived from each data type with observed severe weather reports. These relations are then used to forecast severe weather in independent cases. The results of this experiment show the correlation of severe weather predictors with observed severe weather for both data sets. An estimate of the forecasting potential of the satellite data, relative to the operationally used radiosonde data, also result from this study.

The VAS (VISSR Atmospheric Sounder) is operational on the GOES-4 and GOES-5 (geostationary) satellites (Smith et al., 1981). From the GOES-5, this instrument is sounding the atmosphere with 12 infrared channels nearly every hour. The method of calculating temperature and moisture profiles with the VAS satellite is very similar to that used for the soundings obtained from the NOAA-6 satellite considered in this study. Data from a single VAS observation time should have the same usefulness in forecasting severe weather as a NOAA-6 overpass. Thus, continuous soundings during the day from the VAS satellite should have a great value for monitoring the potential severe weather. A case study using VAS data from several times during the day is shown to demonstrate this point.

The severe weather reports used as predictands in this study were taken from listings compiled weekly by the Severe Local Storms Center in Kansas City, Missouri. The definition of the severe weather listed is the occurrence of one of the following:

- Tornado
- Hail 3/4 inches diameter or more
- Convective surface gust of 50 kts or more.

The time of the reports included were such that they occurred after the valid time of the satellite data. This time varied slightly, from roughly 1300 GMT over the east coast, to slightly after 1500 GMT over the plains. This is due to the orbit of the NOAA-6 satellite which passes over the eastern U.S. at an earlier time. Fortunately, there is usually very little severe weather activity during this time of day, so there was never any doubt as to whether the severe report occurred before or after the satellite observations. The cutoff time of 0800 GMT was somewhat more arbitrary. It is late enough to include severe events which had their origins in daytime heating and destabilization processes.

In order to relate the observed weather to analyzed gridpoint values of the predictors, the severe reports were converted into gridpoint values. The radius of each event was somewhat arbitrarily chosen to be a circle with a radius of two grid units, or approximately 220 km. This expansion of an event covering only a few miles is necessary due to the large scale of the atmospheric observations, especially the spacing of the radiosonde stations. The physical

processes that eventually cause a small scale severe weather event such as a tornado cannot possibly be modelled directly from observations several hours earlier, at a horizontal spacing two orders of magnitude larger. Thus, the areal "extent" of the observed event is made larger to compare with the scale of the observations. The two degree radius corresponds well with other studies of severe weather, and is very close to the same size used by SELS to verify the operational outlooks (Weiss, et al., 1980).

2. NOAA-6 polar orbiting satellite data

NOAA-6 orbits the earth every 102 minutes at an altitude of approximately 1000 km. From this height it is able to scan a swath approximately 2000 km wide. The characteristics of the NOAA-6 sun-synchronous orbit cause it to pass over the eastern United States at roughly 1300 GMT and the plains at 1500 GMT, or the midwest around 1400 GMT (Figure 1). Thus, the NOAA-6 satellite gathers upper air data a few hours after the 1200 GMT radiosonde observations. The availability of soundings at this slightly later time of day should provide a forecast advantage. Also, by the time of the NOAA-6 overpass, it is more likely that boundary layer effects, such as convective mixing due to surface heating, will be felt in the lowest layer (1000-850 mb) of the atmosphere measured by the satellite.

The data available for this study included 36 cases of NOAA-6 sounding data from the spring of 1981, during the period March through June. Each case selected had at least one severe report. With two exceptions, each "case" occurred on separate days. On two days, NOAA-6 passed over the eastern United States as well as the plains states during the next orbit, and there occurred at least one severe weather report within the area observed in each pass.

In order to make a representative comparison of the quality of radiosonde and satellite data, a few restrictions were placed upon the cases selected. Since this study uses objective gridpoint analyses, the density of data and the geometrical dimensions of the area of available data were considered. Five cases were not selected from the 36 available satellite cases. Of these five cases, three were rejected because of excessively large data voids due to extensive cloud cover. The current technology does not allow one to observe the moisture profile through clouds. In this study, only radiosonde and satellite data with comparable data density are compared. Thus, the size of the largest circle one can fit between the radiosonde stations at Green Bay, Wisconsin, St. Cloud, Minnesota, Omaha, Nebraska, and Columbia, Missouri, was calculated. The diameter of this circle is 5.4 degrees latitude, the largest data gap in the radiosonde network east of the Rockies. The satellite cases retained had "holes" due to cloudiness of this same size or smaller.

Two cases were rejected due to their relatively small areal extent east of the Rockies. In this study, there is no attempt to explain the occurrence of severe weather due to topographic effects. Therefore, any data west of 104°W longitude were excluded, thus eliminating severe weather caused directly by mechanical forcings.

3. Successive graphical regression technique

The technique of "successive graphical regression" used to develop the forecasts is described in Panofsy and Briar (1965). It is an empirical method

of establishing non-linear relationships between a predictor and the predictand (in this case the probability of severe weather), as well as non-linear relations using more than one predictor.

Given a number of predictors, successive graphical regression successively maps the values of pairs of predictors into one value, which in this case is the percent chance of severe weather. This percentage is determined empirically from a dependent data set for every observed class interval combination of the pair of predictors. The resulting percentage values are treated as predictors themselves, and are again paired together. The percentage chance of severe weather, given the "new" predictors, is again based upon the dependent data sample relations. A flow chart of the successive non-linear graphical regression technique is shown in Figure 2.

In this study eight individual predictors were selected from both the radiosonde and satellite data. The predictors were divided into pairs. For example, the best two predictors from the satellite data are the Showalter stability index and the 850 mb gradient wind speed. For every observed combination of the seven categories allowed each of these two predictors, the percentage chance of severe weather was tabulated from the "dependent" sample days of this study. This procedure was also followed for the third and fourth best predictors, the 300 mb wind speed and the "shear term," as well as the other two pairings of predictors. The percent chance of severe weather from the first two predictors, the Showalter index and 850 mb wind speed, was then treated as a "new" predictor. This "new" predictor was then grouped with the "new" predictor determined from the "shear term" and 300 mb wind speed pair. For every observed combination of these "new" predictors, an updated percent chance of severe weather was again tabulated from the dependent sample results. The "predictors" are now reduced from eight to four, and these four predictors are mapped further into two predictors. The final two predictors, each of which are a combination of four of the original predictors, are combined into one final percentage probability of severe weather. Figure 2 is a flow chart illustrating the concept of graphical regression.

This scheme accounts for linear and non-linear interactions of pairs of predictors. Twelve predictors were used in this study, and there are 66 possible combinations of twelve predictors taken two at a time. Given a number of predictors, they can be arranged into many different pairs. Thus there is not a unique determination of the probability of severe weather by this method. A search for the "best" combination of predictors is necessary. Thus, for each of the 66 possible unique pairs of predictors, a table of severe weather probabilities was calculated. To evaluate which pairings have the most "value," the "computed information ratio" Ic (Holloway and Woodbury, 1956) was calculated. This value ranges from zero (no information) to one (complete information). The equation for the computed information ratio is:

$$I_c = \frac{\sum_{i=1}^{k}\sum_{j=1}^{l} O_{ij}\ln O_{ij} - \sum_{i=1}^{k} S_i \ln S_i + \sum_{j=1}^{l} S_j \ln S_j + N\ln N}{N\ln N - \sum_{i=1}^{l} S_i \ln S_i}$$

or

$$= 1 - \frac{\sum_{i=1}^{k} S_i \ln S_i - \sum_{i=1}^{k} \sum_{j=1}^{l} O_{ij} \ln O_{ij}}{N \ln N - \sum_{j=1}^{l} S_j \ln S_j}$$

The computed information ratio is valid for a "contingency" table, as shown in Figure 3. The number of predictand categories "l" is always two (severe or non-severe). Considering a single predictor, the number of class intervals "k", for each predictor, is seven in this study. When a pair of predictors is combined into one predictor, k becomes 7 x 7 = 49 different categories. The number N is the total number of dependent data points, 7959 in this study, and is determined by adding either the Si's or Sj's. Sj is the sum of events in the predictand category. In this study, j=1,2 and are the number of non-severe and severe events (gridpoints) in the dependent sample. These values are constant and are 6802 non-severe and 1157 severe events. Oij are the frequencies for a given class of predictor and predictand. The values Si are the sums of the Oij in a given predictor class or row. The values Oij and Si must be tabulated for each contingency table based on a pairing of two predictors. The values Sj and N are constant values, based only upon the frequency of severe and non-severe events in the dependent data set.

Thus for each of the 66 possible predictor pairs, there was an associated Ic. The best pair of predictors was found according to their Ic value and selected for use. From the remaining 10 of the original 12 predictors, the next best pair was selected, again on the basis of the largest Ic. The best eight predictors were selected in this manner, and used in the total graphical regression scheme.

In this way, the maximum possible information content is preserved in this forecast scheme. The predictors used for the radiosonde data are chosen independently from the satellite derived predictors. The Ic of the final table, used to forecast severe weather, appears to be strongly correlated to the original values of Ic valid for the original four pairs of predictors. Specifically, if one pair of predictors is replaced by a pair with a slightly better Ic, the "final" value of Ic will also be slightly improved.

This method was chosen to forecast severe weather after other more conventional methods were tried. The often used technique of stepwise multiple linear regression was found to be unsuccessful. Very little explained variance was found by that technique with the data in this study, as was found also by Miller and David (1971). Evidently linear combinations of predictors do not easily account for the non-linear processes that determine the occurrence of an observed severe storm event. Thus, a non-linear technique was selected for severe weather probability forecasts.

4. Description of severe weather predictors used

Predictors used in this regression scheme include many of the standard ones outlined by Miller (1972). These predictors are the ones used operationally

today. They include a stability parameter, wind speeds at various levels, wind shear, vorticity advection, and parameters that indicate the location relative to the upper level jet. Also included are 8 hour advective temperature and dewpoint changes at 850 mb, and the temperature advection at 500 mb.

The predictors used in this study are:

1. Showalter index ≡ the difference between the air temperature at 500 mb and 850 mb and that of an 850 mb parcel lifted dry adiabatically to lifted condensation level, then moist adiabatically to 500 mb.
2. Change of the Showalter index ≡ (8 hour forecast Showalter) - (observed Showalter).
3. 850 mb wind speed.
4. 500 mb wind speed.
5. 300 mb wind speed.
6. 850 mb temperature advection.
7. 850 mb dewpoint advection.
8. 500 mb temperature advection.
9. "Shear term" of the SWEAT index ≡ 125*(.2+sin(angle between 850 and 500 mb velocity vectors)).
10. 500 mb vorticity advection
11. 300 mb wind speed advection
12. 300 mb horizontal wind speed shear = $\Delta(V)/\Delta s$, s = horizontal distance.

Of these twelve predictors or indices, six are listed explicitly in the AFGWC Technical Report 200 (Miller, 1972). Several of them are included in the "SWEAT" index of Miller et al. (1972). The SWEAT index is a convenient parameter which combines the instantaneous stability of the atmosphere with the 850 and 500 mb wind speeds and directions which imply subsequent changes in stability. The formula for the SWEAT index is:

$$20(TT-49)+12(Td)+2(850\text{ mb speed})+(500\text{ mb speed})+125*(\sin\alpha)+.2)$$

where α is the angle between the 850 and 500 mb wind vectors, and no term is allowed to be less than zero.

Wind speeds from three different levels, 850, 500, and 300 mb, considered in the Miller list, are also studied here. The wind speeds are indicators of energy available for severe storms. Higher speeds are usually associated with a higher likelihood of severe weather, especially tornadoes. Gradient winds are calculated from the satellite derived height fields, and treated in the same manner as radiosonde winds. The statistical scheme used here will yield a quantitative estimate of the relative forecast skill of wind speeds for the three levels.

The 850 and 500 mb wind speeds are two terms which appear in the SWEAT index. In addition to the wind speeds, the directional wind shear is a factor which appears both in the SWEAT index and the Miller list.

Three advection parameters are considered as quantitative predictors in this study; 850 mb temperature and dewpoint advection, and the 500 mb temperature advection. These are the advective changes of the same parameters that are most commonly used to define the stability of the atmosphere, thus quantitatively estimating the future change of stability. Previous studies have been done which have qualitatively mentioned the importance of each of these

advective components. Many of these are summarized by Barber (1974). This study will yield a quantitative comparison of the importance of each.

The advection calculation used is the instantaneous advection computed by the dot product of wind velocity and the gradient of temperature or dewpoint:

$$\vec{V} \cdot \nabla_p T$$

or

$$T = T_o = \vec{V} \cdot \nabla_p T \cdot (\Delta t) \ .$$

The units of both temperature and dewpoint advection calculated in this way are degrees per unit time. Since this study uses data from the early morning hours, several hours before the peak time of occurrence of severe weather, the time interval (Δt) multiplying the advection values was chosen to be equal to eight hours, implying an eight hour forecast of the temperature and dewpoint fields. This assumption of an eight hour interval between the severe weather atmospheric state and the time of the observations is of course only valid in a mean sense but nevertheless are shown to be valid predictors of severe weather. The "eight hour" advection forecast values are also combined with the Showalter index in this study to calculate an advective forecast of the Showalter index.

Specifically, the change of the Showalter index is constructed from the difference of the actual index and the "forecast" index due to advection. If $\Delta T(850)$, $\Delta T(500)$, and $\Delta Td(850)$ are the advective changes of temperatures and dewpoints as described above, the forecast Showalter index is calculated from the following "new" temperature and dewpoint fields: $T_o(850) + \Delta T(850)$; $Td_o(850) + \Delta Td(850)$; and $T(500) + \Delta T(500)$. The change of stability is the difference between the "forecast" and the original Showalter indices. While the values obtained in this way may be unrealistically high due to the assumption of unchanging advection, it is still valid in a statistical sense to use this quantity as a predictor.

Whitney (1956) found that the location of severe weather occurrences correlated not only with the Showalter index, but also with the forecast change of the index. Whitney used 1200 GMT radiosonde data to make an eight hour trajectory forecast of the components of the Showalter index.

From the standard radiosonde winds and the previously described satellite gradient winds, four dynamic (wind related) predictors are calculated. They are the "shear term" of the SWEAT index, the 300 mb horizontal speed shear, 500 mb vorticity advection, and the 300 mb wind speed advection. The advection quantities are calculated with the same instantaneous formulation as the temperature advections.

The "shear term" of the SWEAT index is the vertical wind shear, an important ingredient for severe weather. The value is proportional to the sine of the angle between the 850 and 500 mb wind vectors, with "veering" winds considered positive (favorable to severe weather). The exact formulation of this term is: $(125*(\sin \alpha)+.2)$. In the original design of the SWEAT index, this shear term is set to zero if it is negative or if the wind speed is less

than 15 knots. In addition, the direction of the wind at both levels has restrictions. The 850 mb wind must be from between 130 and 250 degrees (i.e., a strong southerly component), and the 500 mb wind must be from between 210 and 310 degrees (a strong westerly component). If either of these directional conditions are not met, the whole term is set equal to zero. Values for the term range from 0 to +150, with the large positive values being most favorable for severe weather.

For the purpose of a statistical prediction scheme, some modifications of the shear term were desirable. The modifications allow the term to have values distributed over a larger range, and largely alleviate the cluster of values at zero. The "negative" angles, or backing winds, were allowed to yield a negative shear term. With this modification, another lesser modification followed. It is possible to have 850 and 500 mb winds from the southwest, between 210 and 250 degrees, that, according to the original SWEAT index, qualify individually but not together if the angle between them is "negative." For this occasional occurrence, small "negative" angles were set equal to zero. A further modification for this study required that the wind speeds at both levels exceed only 3 meters per second or 6 knots, as opposed to the original 15 knots. Figure 4 shows the wind directions and shears allowed on the original form of the SWEAT index, and the changes in this study.

According to the omega equation, positive vorticity advection at 500 mb is generally associated with rising vertical motion. If a stable layer of the atmosphere is lifted, it becomes less stable, and more favorable for severe weather.

The horizontal wind shear at 300 mb is another parameter on the Miller list. This upper level shear is related to relative vorticity, and if positive, favorable to severe weather. This parameter is also a measure of the relative position to the jet core. The maximum value of shear is found to be at the edge of the jet core, a position which may be more favorable to severe weather than the middle of the jet core. In combination with the other parameters, this predictor is valuable in relating the occurrences of severe weather to the location of the 300 mb jet streak.

Another parameter relating severe weather to the position of the jet stream is the 300 mb speed advection. This parameter will be an indication of the leading edge, or the exit region of the jet. It has been shown (Uccellini and Johnson, 1979) that the exit region of the upper level jet induces lower level secondary circulations, leading to a thermal destabilization favorable to severe weather.

5. Satellite sounding calculation

The method of solving the radiative transfer equation for temperature and moisture retrievals was the "general iterative" method (Smith, 1970). A current LFM forecast of temperatures and dewpoints, valid at the time of the satellite pass, was used as a first guess. From this first guess, the expected radiance to space of the various channels is calculated. These radiance values are checked against the values observed by the satellite. If the expected radiance values do not agree within the expected observation noise, the guess temperature profile is changed so as to produce better agreement with the observed radiances. The process is repeated until the radiances calculated from the

"retrieved" temperature profile and those observed from the satellite agree within a convergence limit proportional to the noise level of the radiometer measurements.

Interactive Editing of Retrievals

Retrievals were made from the NOAA-6 satellite using the McIDAS (Man-computer Interactive Data Access System). Retrievals are attempted by the computer at regularly spaced intervals, after which the meteorologist may both add to the existing data and edit the total data set (Smith et al., 1978).

An automated chain of computer software attempts soundings at approximately 75 km intervals using 3 x 3 fields of view of the HIRS (High resolution Infrared Radiometer Sounder) aboard NOAA-6. Cloudiness affects the probability of success of retrievals attempted at these regularly spaced intervals. In areas where the cloud cover is very heavy, very few retrievals are possible. In partly cloudy areas, the automatic selection of retrieval locations often did not choose the optimal or clearest field of view. In areas of potential severe weather, it may be desirable to have more data than the 75 km density already given by the computer.

A meteorologist can control the McIDAS to calculate additional retrievals in the areas deemed data sparse due to the above reasons. He is able to obtain a better data density, especially in partly cloudy regions. The ability of McIDAS to display rapidly data of many types allowed him to determine areas of possible severe weather. Parameters such as stability indices, winds, as well as other conventional data types were used to locate these areas. Many sources of data were available to the meteorologist, including the satellite retrievals being processed, as well as the radiosonde data, the conventional surface network, and real time GOES images.

After one has as many retrievals as desired, it is necessary to screen or "edit" the data to ensure meteorological consistency from one sounding to the next. The objective checks performed on individual retrievals are not sufficient to guarantee this consistency. Cloudiness, humidity, high terrain, and the surface skin temperature can cause the retrieval solutions to have localized errors.

Using the analysis and display capabilities of McIDAS, the meteorologist can examine the satellite retrievals in the form of parameters he is familiar with. These parameters are temperatures, dewpoints, heights, and thermally derived gradient winds at any of the mandatory pressure levels. Also available for examination are analyses and plots of thicknesses and precipitable water. Examining these parameters, the meteorologist can successfully edit the set of retrievals to obtain a subset that is meaningful for diagnosing synoptic or subsynoptic scale meteorological processes.

It may seem possible through the editing process to select a subset of satellite retrievals fitting into some preconceived pattern; however, this is not the case. The data in this study have an average horizontal density of data at least five times greater than that provided by the radiosonde network. In cases with plentiful data, it is not possible to alter the locations of any isopleth by removing a few erroneous reports. The editing guidelines followed were largely due to the characteristics of the Barnes (1973) and Cressman (1959)

objective analysis methods of analyzing the data to gridpoints. The most typical reason for deleting a satellite sounding is merely to remove a very small scale "noise" wave produced in an isopleth generated by a very sensitive analysis scheme.

6. Results

a. Division of data into dependent and independent sets

Thirty-one "cases" of NOAA-6 sounding data from the spring of 1981 with corresponding radiosonde data were available in this study. In order to properly divide the data into representative dependent and independent data sets, the cases were arranged in order of the number of severe weather reports. With the cases in this order, every third case was chosen to be an "independent" case, and the rest to be "dependent" data. Thus, both the dependent and independent data sets consist of a widely varying range of meteorological situations, ranging from isolated occurrences of severe weather to major outbreaks with up to 54 reports in one day.

b. Dependent data

The graphical regression technique used in this study shows the relative importance of predictors commonly used in forecasting severe weather. This study also shows that the overall skill using satellite soundings in forecasting severe weather is as high as that of currently used radiosonde data.

Tables of the computed information ratio, Ic, based on the dependent data set show the relative value of the severe weather predictors considered in this study. The diagonals of Tables 1 and 2 contain Ic values for predictors considered singly, while the Ic values of two predictors used together are shown in the rest of the tables.

The relative order of value of predictors used singly is listed separately in Tables 1 and 2. It is seen that the stability index is the best predictor for both radiosonde and satellite soundings. The relative order of predictors is similar in both the satellite and radiosonde data sets. The largest difference between satellite and radiosonde derived predictors is the level of wind speed best correlating with severe weather. The satellite shows the 850 mb level wind speed to correlate best, while the 500 mb radiosonde wind speed is the level which contains the most information concerning severe weather development.

The similarity of the two types of data is even greater when predictors are used in combination. For the regression scheme used in this study, the pair of predictors with the highest computed information ratio in Table 1 (or 2) was selected for use. With these two predictors excluded, the pair of predictors with the next highest value of Ic was selected as a predictor. This process was repeated until four predictor pairs consisting of eight different single predictors were chosen. The predictors selected in this way for satellite and radiosonde data are listed in Tables 1 and 2.

It is seen in these tables that the same eight predictors were selected out of the twelve available for each data type. Using either satellite or radiosonde soundings, the "best" predictors consist of the Showalter index, wind

speeds, vertical wind shear, and temperature advections. The only significant difference between the satellite and radiosonde predictors selected for inclusion in this forecast method is the skill of the 850 mb wind speed relative to the other predictors.

An exceptional improvement is seen in the information ratio value of the satellite Showalter index over that of the radiosonde Showalter index. The satellite derived Showalter index has a computed information ratio value of .125 versus .101 for the radiosonde derived index. This difference is most likely due to the higher density of the satellite sounding data. Since most of the variation of a stability parameter is determined by the variation of the moisture field, it is clear that the horizontal detail of the moisture field is better seen from the satellite soundings.

c. Independent data forecasts

Using the graphical regression method, forecasts of severe weather for 10 independent days were made, using first radiosonde then satellite data. Forecast severe weather probability values were calculated for each gridpoint of a set of analyzed predictors. Threat scores, as well as the probability of detection (POD), false alarm ratio (FAR), and the reliability, were calculated for the independent forecasts. Derivations of the first three of these can be found in Weiss, Kelly and Schaefer (1980).

The POD can be written as

$$X/(X + Y) ,$$

and the FAR is

$$Z/(X + Z) ,$$

where X=area verifying severe correctly forecast severe, Y=area verifying severe but not forecast severe, and Z=area forecast severe not verifying severe.

The threat score is a combination of the POD and FAR scores, and can be written as:

$$X/(X + Y + Z) .$$

The POD and threat scores range from 0 (worst forecast) to 1 (perfect forecast), while the best FAR score is 0 and the worst possible is 1.

To compute these scores, a threshold value of a predictor, here the probability of severe weather, must be selected. A range of values was tested to find the probability that achieved the highest scores. In this study, a value of approximately 20 percent was found to be the best threshold value for both satellite and radiosonde data.

Values of the threat score, POD, and FAR are shown in Table 3 for different threshold values of the predicted percentage chance of severe weather. Using the best percentage threshold of 20 percent, satellite soundings showed threat scores equal to or slightly better than the radiosonde data.

The "reliability" of the probability forecasts is shown in Figure 5. The forecast percentages are graphed against the observed frequency of severe weather in the independent data set. Perfect forecasts would lie along the straight diagonal line, meaning that the probability of severe weather could be forecast perfectly. Points plotted in the diagram are the midpoints of the 12 percentage categories used in this study. As may be seen for 9 of the 12 categories, satellite data provided a probability forecast more likely to be realized than the radiosonde forecast.

d. May 23, 1981 example

Maps of the percentage probability of severe weather for May 23, 1981, calculated from the predictor grids, are shown in Figure 6. A large outbreak of severe weather occurred on this day with 54 total reports. Only the area with a severe weather probability forecast of 20 percent or greater is considered, as this value provided the best threat score overall. For purposes of display, a band filter removing small scale features less than 100 km was applied, resulting in smoother contours. Note that the graphical regression method results in a map which is comparable in size and shape to operational outlooks of severe weather.

On this particular day, the radiosonde data over-forecast the area of actual severe weather. For example, southwestern Wisconsin and northeastern Iowa, where there is no radiosonde data, should not have been forecast severe. The higher spatial density NOAA-6 satellite data were able to outline the extent of severe weather more closely in this region, although a few reports lie outside of the region forecast to be severe by the satellite.

Areas of distinctly high probabilities of severe weather can be seen in both data sets. These areas are those where several predictors are favorable to severe weather, which are allowed by the graphical regression technique to interact non-linearly yielding high probabilities of severe weather.

The cluster of severe reports in Missouri is accurately defined by the area of high probability values indicated by both the satellite and radiosonde forecasts. The large number of reports in Iowa corresponds very well to the maximum probabilities derived from the radiosonde data. The forecast maximum of 60 percent from the NOAA-6 data accurately pinpoints the cluster of tornadoes and large hail reports which verified in Oklahoma. In this example the number of severe weather reports is higher near those areas with higher percentage forecasts, as suggested by the reliability diagrams.

e. Example application from VAS, the geosynchronous sounder

A case study from the spring of 1982 with VAS data from several morning and early afternoon time periods is included to further demonstrate the graphical regression method, and to show the potential of the VAS data for providing additional information valuable to updating severe weather forecasts. The case is May 21, 1982, when severe weather occurred from Texas to Iowa to Tennessee. Forecasts were made using VAS data from four times during the day, before the severe weather occurred.

The area forecast to have a 20 percent or greater probability of severe weather using 1400 GMT VAS data (Figure 7) changes little through the day. This demonstrates the consistency and reliability of the VAS data and the graphical

regression forecast method. Many severe weather reports did indeed occur from Arkansas to Kentucky, in the area common to all forecasts.

The forecast probability values over Texas, however, showed a large increase with time from low values to values well over the 20 percent threshold. Severe weather did indeed occur in Texas, verifying the later forecasts. Figure 8 shows how the Showalter index varied through the day as measured by VAS. The rate of decrease of stability over initially unstable Tennessee and Kentucky was fairly slow but steady. A more rapid decrease was seen over Texas. In this case, early observed values from the VAS soundings of the time rate of change of the stability, as well as the rate of change of other predictors, could have significant effects upon the forecasts. These time change predictors will be considered in future studies.

7. Summary and suggestions for future work

This study indicates that satellite derived data have information comparable with the radiosonde data with regard to forecasting severe weather. Using satellite and radiosonde data separately, a slightly higher threat score is achieved from the satellite data. In general, most of the satellite parameters taken individually are slightly less valuable predictors than their radiosonde counterparts, according to the Ic values in Tables 1 and 2, although the information content of all predictors taken as a group is about the same.

Although the relative value of the predictors to each other is approximately the same from radiosonde data to satellite data, there are two notable exceptions. The satellite derived stability index shows a much higher correlation with severe weather than the conventional radiosonde data. The reason for this is likely due to the higher data density of the satellite data. This density allows the peak values of the stability field to be geographically positioned more accurately, which is perhaps mostly from the increased detail of the moisture field. The satellite 500 mb gradient wind speed showed poor skill relative to the other wind levels and to the radiosonde data. The fact that the 500 mb level is the poorest correlating level for satellite data may be related to the satellite data's poorer vertical resolution. The relatively good skill of the satellite 850 mb wind is most likely due to the fact that the gradient wind calculation is highly correlated to the surface temperature and pressure fields which are provided accurately and with good resolution in both time and space. The high correlation of the satellite's 300 mb gradient wind probably results from the fact that it is based on a deep layer mean temperature gradient.

The technique of successive graphical regression seems appropriate for application to the severe weather forecast problem. The addition of additional predictors never lessens the information content of the method. Nonlinear characteristics of severe weather are seen in many of the individual predictors, as well as in the combination of predictors.

Suggestions for future work

A number of refinements to this study are need to improve the reliability of this forecast method. First, the data set should be expanded to another severe weather season. For purposes of forecasting severe weather on an operational basis, the predictors should include many sources besides upper air

parameters, including surface data, numerical model data, and geographical and diurnal climatology. With the VAS (VISSR Atmospheric Sounder) instrument, soundings on an hourly basis will allow the observed time change of any of the predictors included in this study. A combination of the satellite and radiosonde predictors would certainly result in better forecasts than either data set alone. It is likely that the radiosonde data would be used to determine many of the absolute values of the predictors, and the VAS satellite would provide many valuable time changes of these parameters.

The predictors used in this study were basically very "traditional," and many variations of them are possible. The graphical regression technique could also be used with "new" predictors (e.g., radiance gradients), which would be empirical functions of other "basic" parameters. The graphical regression method should be allowed to select temperatures and dewpoints from nearby gridpoints, presumably upstream, that correlate best with future severe weather. The use of predictors at other gridpoint locations will allow the horizontal structure of the atmosphere to be taken into account, especially the horizontal detail available from the satellite soundings. In this way, upstream thermal and moisture tongues and ridges, and "short waves" will have an influence upon a severe weather forecast. These refinements are the objective of future research.

Acknowledgments

Our gratitude is extended to Professor V. E. Suomi, Dr. Paul Menzel, Mr. M. Johnson of the University of Wisconsin, and Dr. John Lewis and Mr. William Togstad of NESDIS for their assistance in this study. Thanks are extended to Mrs. Gail Turluck for preparing this manuscript for publication. This study was supported by the National Aeronautics and Space Administration under contract NAS5-21965.

References

Blechman, A. G., 1981: The influence of higher resolution Nimbus-6 soundings in locating jet maxima. M.S. thesis, Department of Meteorology, University of Wisconsin, Madison, Wisconsin, 53706, 77 pp.

Barber, D. A., 1974: The production of available thunderstorm energy. Ph.D. thesis, Department of Meteorology, University of Wisconsin, Madison, Wisconsin, 53706, 63 pp.

David, C. L., and J. S. Smith, 1971: An evaluation of seven stability indices as predictors of severe thunderstorms and tornadoes. Preprints of papers presented at the Seventh Conference on Severe Local Storms, Kansas City, Missouri, October 5-7, 1971, available through American Meteorological Society, 45 Beacon Street, Boston, Massachusetts, pp. 5-109.

Hayden, C. M., W. L. Smith, and H. M. Woolf, 1981: Determination of moisture from NOAA polar orbiting satellite sounding radiances. J. Applied Meteor., 20, 450-466.

Holloway, L., and M. A. Woodbury, 1955: Application of information theory and discriminant function analysis to weather forecasting and forecast verification. University of Pennsylvania, The Institute for Cooperative Research, Philadelphia, Pennsylvania, 224 pp.

Miller, R. C., 1972: Notes on analysis and severe-storm forecasting procedures of the Air Force Global Weather Central. Air Weather Service Technical Report 200 (rev.), available from Air Force Global Weather Central, Offutt Air Force Base, Nebraska.

Miller, R. C., A. Bidner, and R. A. Maddox, 1972: The use of computer products in severe weather forecasting (the SWEAT index). Aerospace Sciences Review, 72-1, 2-9.

Miller, S. R., and C. L. David, 1971: A statistically generated aid for forecasting severe thunderstorms and tornadoes. Preprints of papers presented at Seventh Conference on Severe Storms, Kansas City, Missouri, October 5-7, 1971, available through American Meteorological Society, 45 Beacon Street, Boston, Massachusetts, 42-44.

Panofsky, H. A., and G. W. Brier, 1963: Some applications of statistics to meteorology. Mineral Industries Continuing Education, College of Mineral Industries, The Pennsylvania State University, University Park, Pennsylvania, 224 pp.

Smith, W. L., 1970: Iterative solution of the radiative transfer equation for the temperature and absorbing gas profile of an atmosphere. Applied Optics, 9, 1993-1999.

Smith, W. L., C. M. Hayden, H. M. Woolf, H. B. Howell, and F. W. Nagle, 1978: Interactive processing of TIROS-N sounding data. Preprints, Conference on Weather Forecasting and Analysis and Aviation Meteorology, Silver Spring, Maryland, October 16-19, 1978, available from American Meteorological Society, 45 Beacon Street, Boston, Massachusetts, 02108, 390-395.

Smith, W. L., H. M. Woolf, C. M. Hayden, D. Q. Wark, and L. M. McMillin, 1979: The TIROS-N Operational Vertical Sounder. Bull. Amer. Meteor. Soc., 60, 1177-1187.

Smith, W. L., V. E. Suomi, W. P. Menzel, H. M. Woolf, L. A. Sromovsky, H. E. Revercomb, C. M. Hayden, D. N. Erickson, and F. R. Mosher, 1981: First soundings results from VAS-D. Bull. Amer. Meteor. Soc., 62, 232-236.

Uccellini, L. W., and D. R. Johnson, 1979: The coupling of upper and lower tropospheric jet streaks and implications for the development of severe convective storms. Mon. Wea. Rev., 107, 682-703.

Weiss, S. J., D. L. Kelly, and J. T. Schaefer, 1980: New objective verification techniques at the National Severe Storms Forecast Center. Preprints of papers presented at the Eighth Conference on Weather Forecasting and Analysis, Denver, Colorado, June 10-13, 1980, available from American Meteorological Society, 45 Beacon Street, Boston, Massachusetts, 02108, 412-418.

Whitney, L. F., 1956: Destabilization by differential advection in the tornado situation of 8 June 1953. Bull. Amer. Meteor. Soc., 38, 353-356.

Table 1

Computed information ratios Ic for satellite data
single predictors (diagonal) and pairs of predictors
Values times 1000

		Satellite predictors											
		1	2	3	4	5	6	7	8	9	10	11	12
1)	Showalter	125											
2)	Delta Showalter	136	4										
3)	850 Temp. adv.	157	36	24									
4)	850 Dewpt. adv.	143	27	40	9								
5)	500 Temp. adv.	140	32	46	29	8							
6)	850 wind speed	160	61	74	71	66	40						
7)	500 wind speed	154	27	49	39	38	70	14					
8)	300 wind speed	158	38	56	45	46	77	34	22				
9)	Vert. shear term	159	56	61	61	56	89	73	80	38			
10)	300 horiz. shear	138	24	45	26	25	59	32	41	62	6		
11)	500 vort. adv.	142	17	46	24	24	56	29	37	60	20	5	
12)	300 speed adv.	145	21	34	22	26	58	31	42	53	20	18	3

Best single predictors in order:
1st - Showalter (1)
2nd - 850 wind speed (6)
3rd - Vertical shear term (9)
4th - 850 temperature advection (3)
5th - 300 wind speed (8)
6th - 500 wind speed (7)
7th - 850 dewpoint advection (4)
8th - 500 temperature advection (5)
9th - 300 speed shear (10)
10th - 500 vorticity advection (11)
11th - change of Showalter index (2)
12th - 300 speed advection (12)

Best predictor pairs in order:

1 and 6

8 and 9

3 and 7

2 and 5

others not used in graphical regression forecasts

Table 2

Computed information ratios Ic for radiosonde data
single predictors (diagonal) and pairs of predictors
Values times 1000

		Radiosonde predictors											
		1	2	3	4	5	6	7	8	9	10	11	12
1)	Showalter	101											
2)	Delta Showalter	129	23										
3)	850 Temp. adv.	136	60	41									
4)	850 Dewpt. adv.	129	31	55	11								
5)	500 Temp. adv.	122	42	71	28	10							
6)	850 wind speed	141	66	78	60	60	42						
7)	500 wind speed	147	68	92	59	53	84	36					
8)	300 wind speed	124	47	73	36	41	75	69	17				
9)	Vert. shear term	150	93	98	85	92	115	121	102	73			
10)	300 horiz. shear	106	30	51	22	17	53	47	30	78	6		
11)	500 vort. adv.	108	25	47	13	15	42	39	31	80	9	2	
12)	300 speed adv.	108	36	54	22	22	46	38	25	82	6	5	

Best single predictors in order:

1st - Showalter (1)
2nd - Vertical shear (9)
3rd - 850 wind speed (6)
4th - 850 temperature advection (3)
5th - 500 wind speed (7)
6th - Change of Showalter (2)
7th - 300 wind speed (8)
8th - 850 dewpoint advection (4)
9th - 500 temperature advection (5)
10th - 300 speed shear (10)
11th - 500 vorticity advection (11)
12th - 300 speed advection (12)

Best predictor pairs in order:

1 and 9

3 and 7

6 and 8

2 and 5

others not used in graphical regression forecasts

Table 3

Threat Score, Prefigurance, False Alarm Ratio
Comparison Table

	THREAT SCORE X/(X+Y+Z) (1.0 = best)				
THRESHOLD	15%	20%	25%	30%	35%
RADIOSONDE	.271	.278	.277	.272	.252
SATELLITE	.270	.283	.269	.251	.205

	PREFIGURANCE X/(X+Y) (1.0 = best)				
THRESHOLD	15%	20%	25%	30%	35%
RADIOSONDE	.779	.704	.613	.526	.423
SATELLITE	.718	.602	.474	.368	.257

	FALSE ALARM RATIO Z/(X+Z) (0.0 = best)				
THRESHOLD	15%	20%	25%	30%	35%
RADIOSONDE	.706	.685	.664	.639	.616
SATELLITE	.698	.651	.615	.561	.494

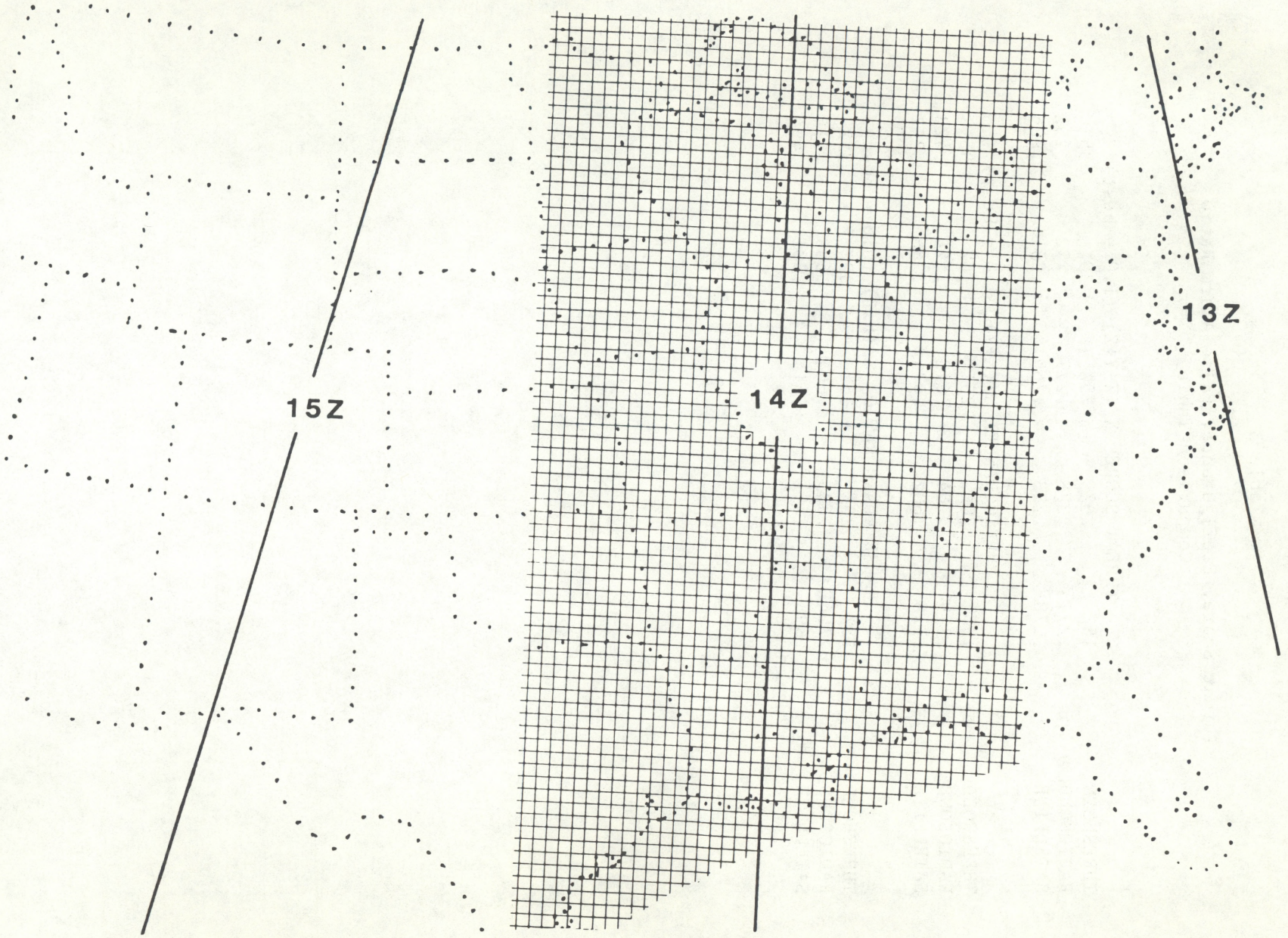

Figure 1.--Approximate times and positions of NOAA-6 overpasses. Shaded area is approximate coverage.

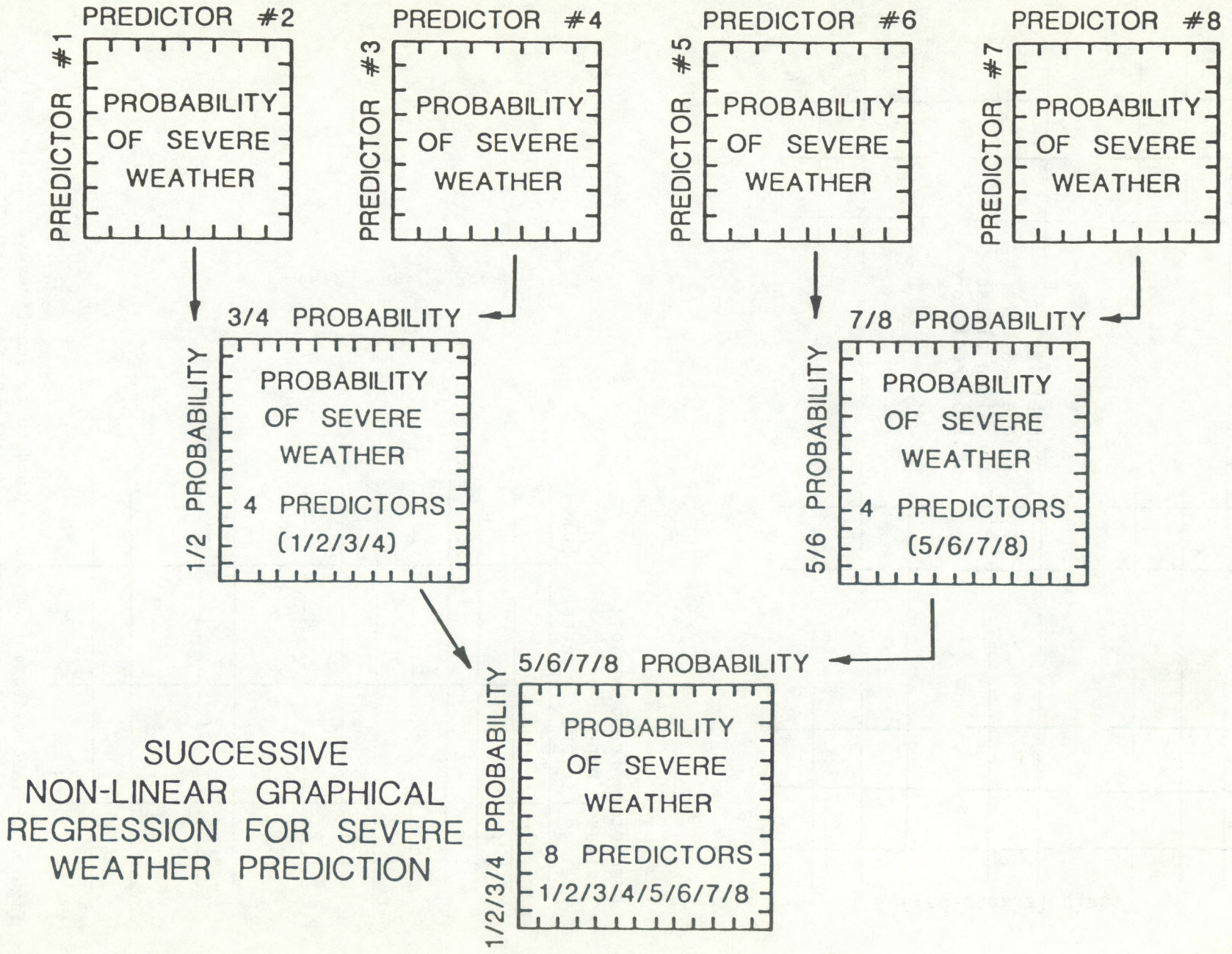

Figure 2.--Graphical regression flow chart.

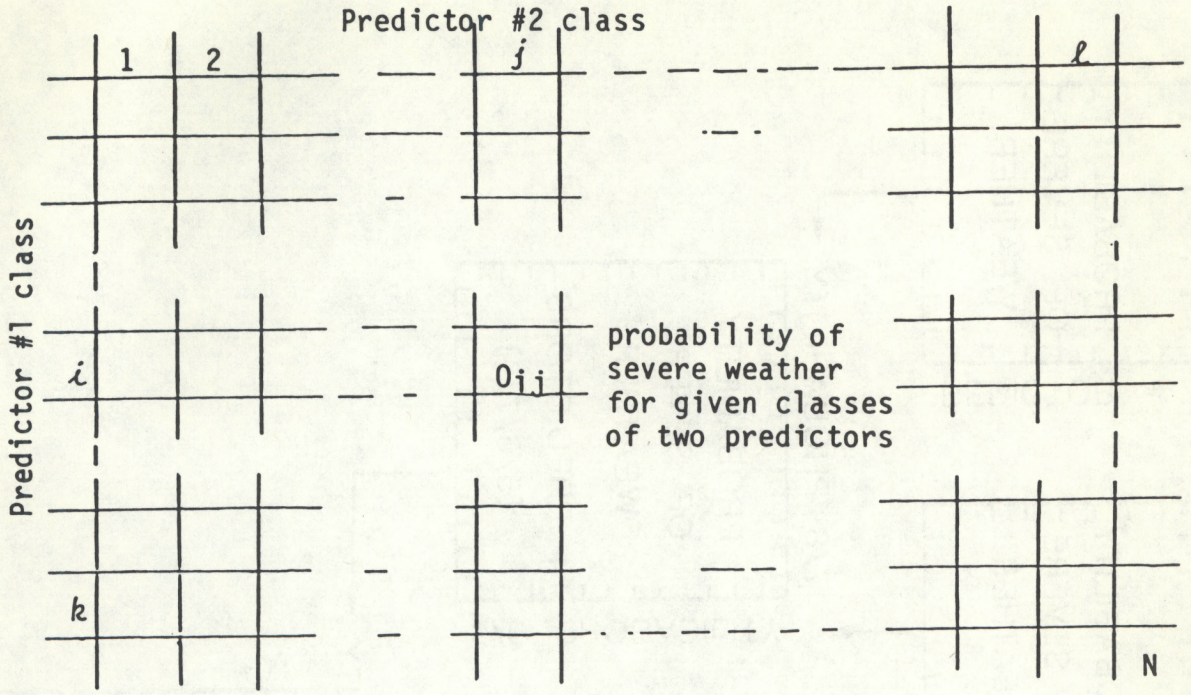

predictor class #1	#2	Frequency of: non-severe	severe	Sums
1	1			
1	2			
1	3			
⋮				
1	k			
2	1			
2	2			
⋮				
"i"row		O_{ij}		S_i
⋮				
k	ℓ			
		S_j	"j"	N

Figure 3.--(Above) Format of tables used to forecast severe weather with graphical regression method. (Left) Same information as above, but in "contingency table" format for calculation of Ic.

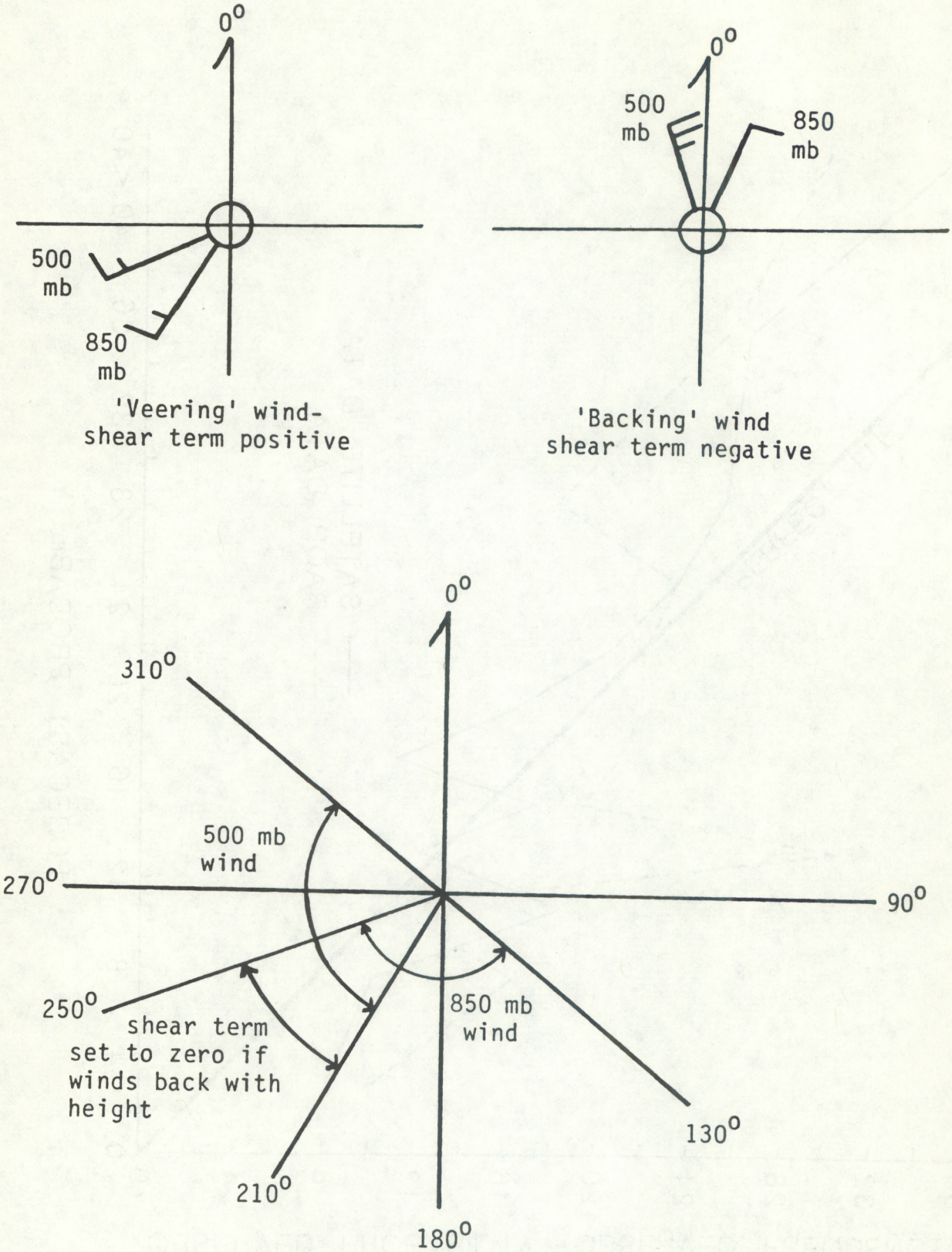

Figure 4.--Original requirements of the 850 and 500 mb wind directions in 'shear term' of SWEAT index; also sector in which this study sets backing wind equal to zero as opposed to a negative value.

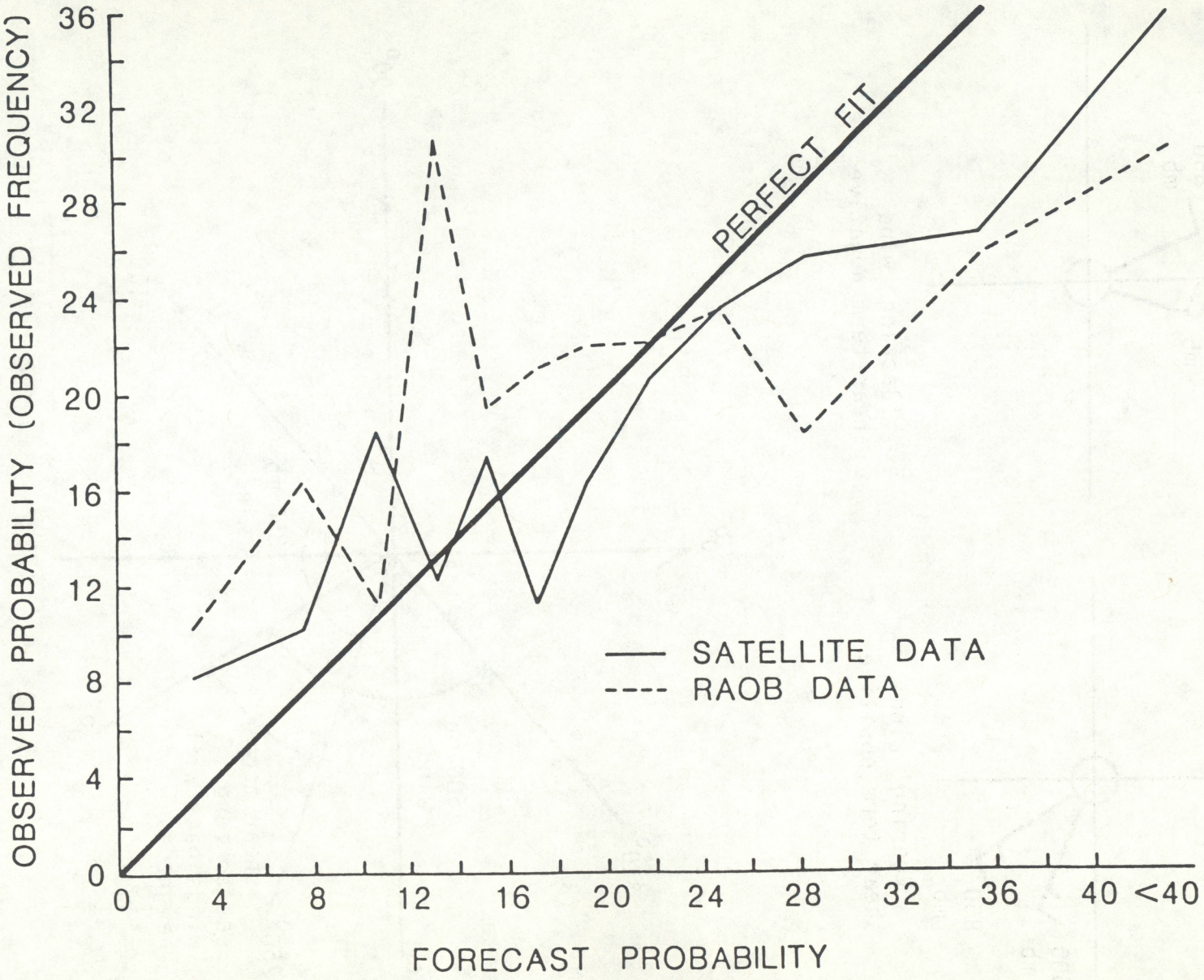

Figure 5.--Reliability diagram.

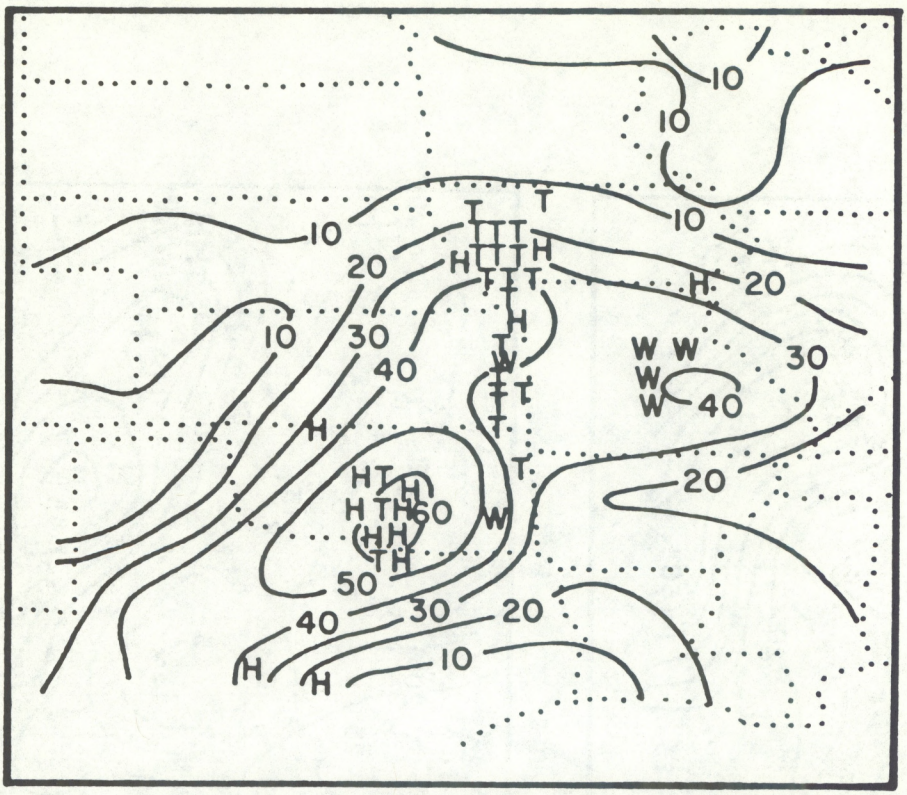

NOAA-6 data

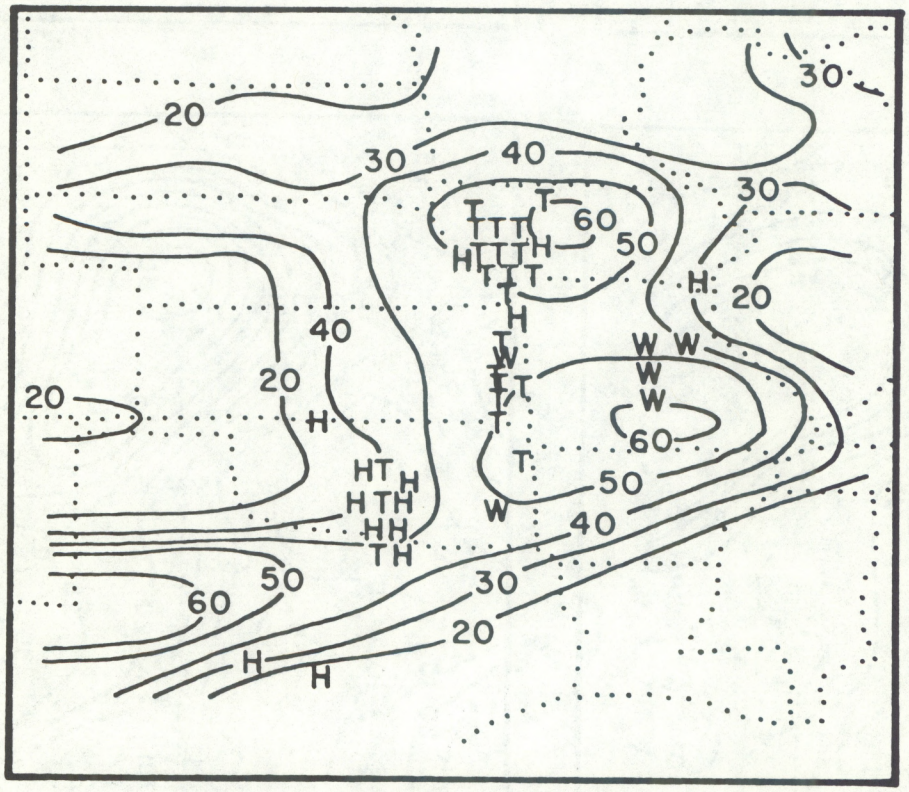

Radiosonde data

Figure 6.--Severe weather probability forecasts for May 23, 1981 using 14 GMT NOAA-6 soundings (top) and 12 GMT radiosonde data.

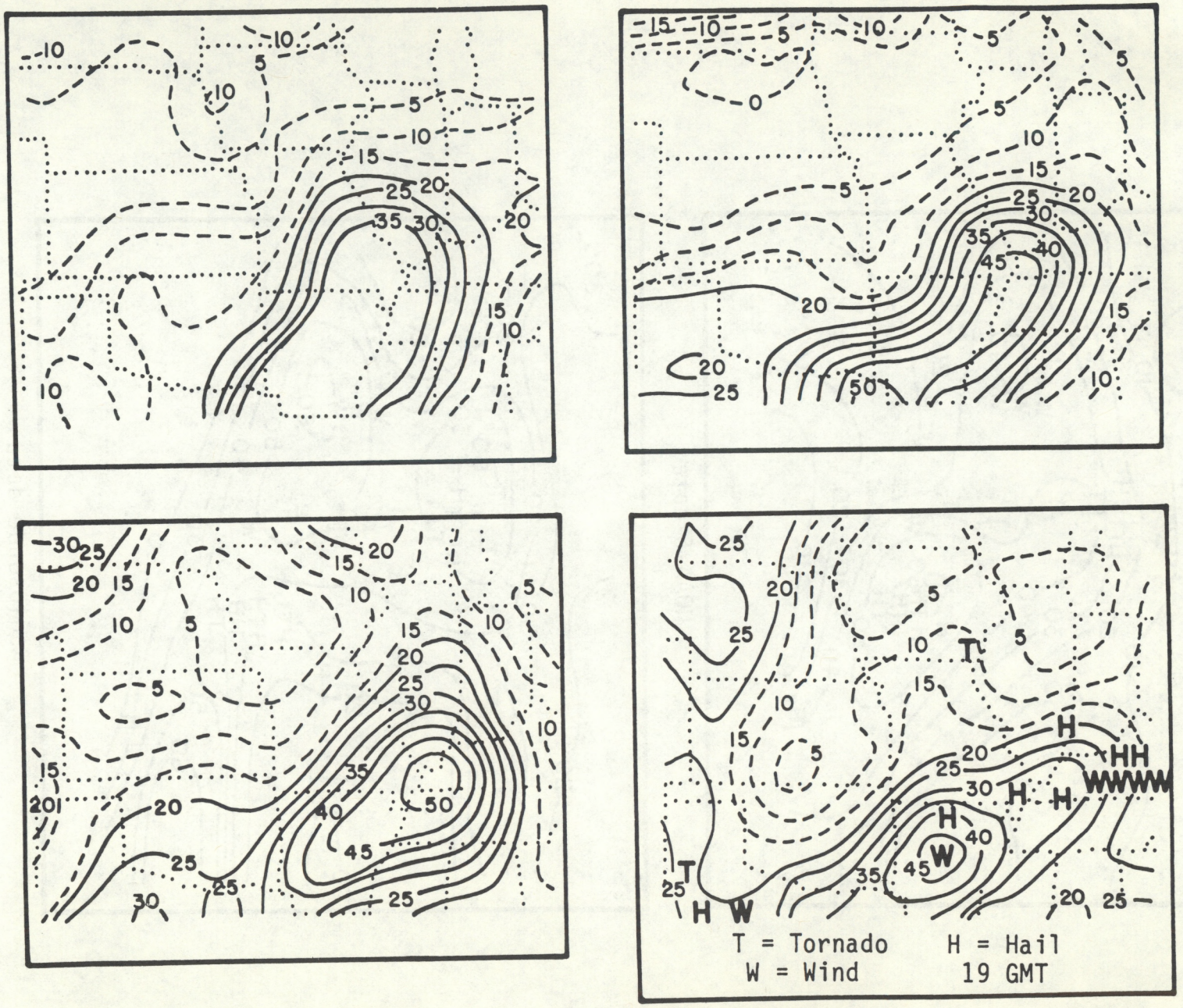

Figure 7.--Forecasts of severe weather probability using VAS soundings from four times on May 21, 1982.

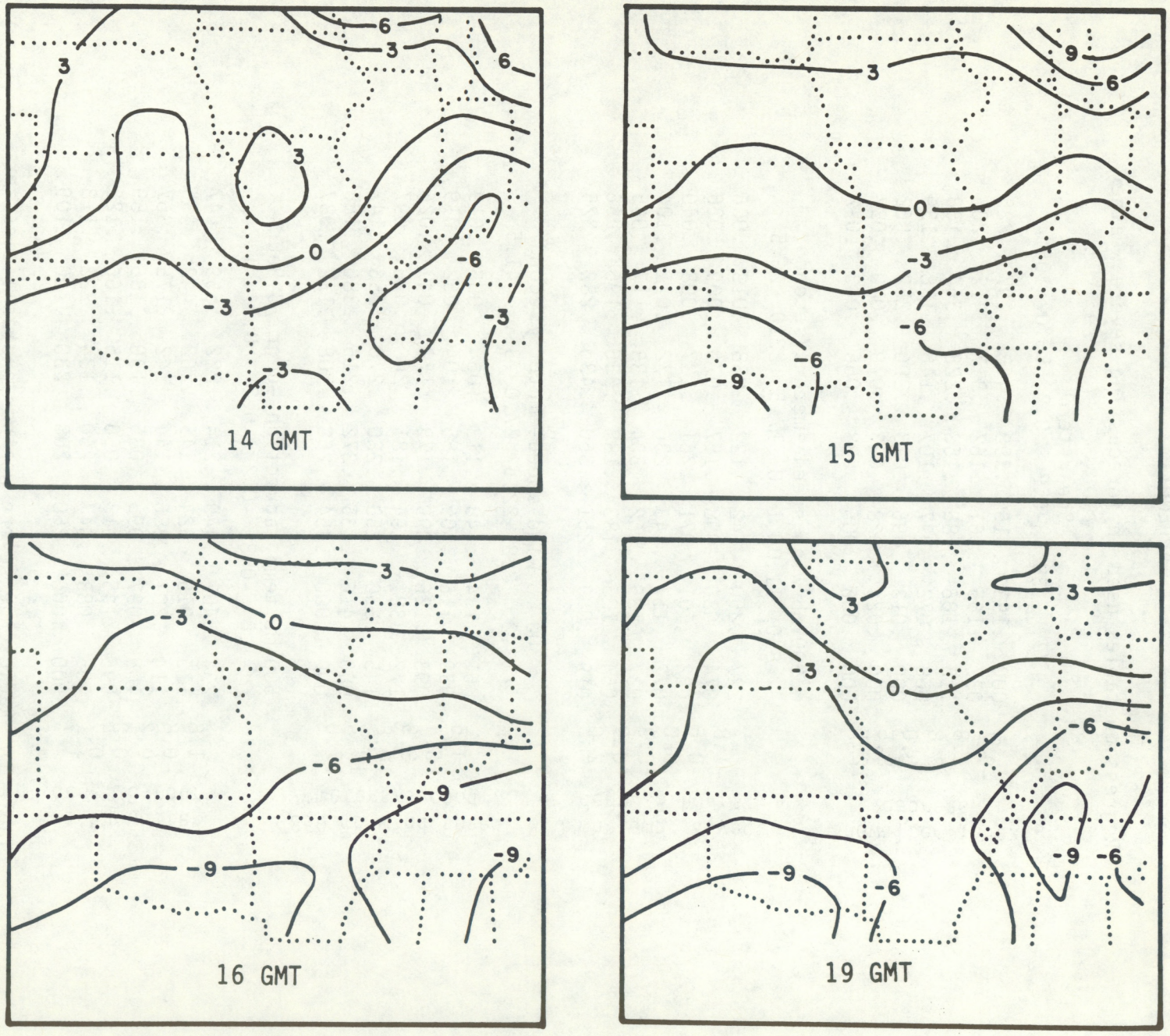

Figure 8.--VAS observed Showalter index at four times on May 21, 1982.

APPENDIX

Regression tables used in forecasting severe weather

Showalter index, degrees	Shear term: -77.	.38.	-0.2	0.2	55.0	105.
-0.7	.000	.193	.415	.390	.468	.297	.225
1.8	.037	.165	.161	.162	.317	.412	.206
3.8	.118	.106	.185	.153	.228	.364	.138
6.0	.068	.072	.097	.107	.146	.188	.139
8.5	.000	.013	.096	.073	.296	.252	.062
12.5	.000	.024	.038	.093	.079	.080	.087
	.000	.006	.006	.038	.066	.063	.072

850 mb temp. advect. degr./8 hours	500 mb wind speed--meters/second: 8.0	11.0	14.0	17.5	22.0	26.5
-1.8	.227	.250	.142	.122	.038	.013	.006
-0.6	.074	.086	.098	.157	.079	.009	.026
0.0	.082	,101	.071	.261	.127	.008	.040
0.3	.072	.117	.143	.236	.172	.071	.104
0.9	.037	.135	.162	.304	.183	.117	.065
2.0	.054	.125	.183	.188	.336	.196	.256
	.019	.089	.251	.360	.430	.282	.325

850 mb wind speed meters/second	300 mb wind speed--meters/second: 13.2	18.2	22.5	27.0	33.5	41.5
4.5	.061	.134	.148	.113	.064	.055	.019
6.4	.039	.116	.109	.155	.104	.052	.019
8.5	.093	.126	.099	.178	.172	.047	.026
10.8	.172	.321	.194	.181	.208	.073	.097
13.3	.145	.330	.258	.280	.270	.256	.142
17.0	.000	.416	.435	.372	.215	.380	.186
	.000	1.000	.454	.258	.108	.132	.087

Δ Showalter degr./8 hours	500 mb temp. advection--degr./8 hours: -1.8	-0.8	-0.2	0.2	0.7	1.7
-1.8	.234	.407	.449	.214	.222	.559	.647
-0.8	.175	.316	.324	.145	.262	.442	.435
-0.2	.114	.207	.286	.144	.142	.175	.367
0.2	.105	.097	.095	.085	.130	.185	.189
0.7	.096	.145	.113	.050	.115	.166	.122
1.7	.105	.083	.047	.250	.134	.222	.118
	.000	.000	.250	.208	.230	.250	.109

Table 1A. Radiosonde severe weather probabilities for given classes of predictors. This table equivalent to top row of figure 2 in text.

Class interval dividers (percent)	Class interval dividers (percentages) .06	.09	.12	.14	.16	.18	.20	.23	.26	.30	.40
.06	.001	.027	.007	.000	.000	.027	.000	.000	.095	.000	.152	.000
.09	.030	.030	.030	.060	.095	.035	.107	.000	.061	.308	.123	.333
.12	.041	.055	.092	.103	.211	.147	.086	.599	.105	.062	.297	.076
.14	.000	.000	.099	.000	.045	.142	.142	.371	.153	.375	.379	.199
.16	.095	.112	.144	.103	.187	.239	.083	.227	.166	.105	.309	.333
.18	.022	.109	.156	.199	.156	.233	.120	1.000	.157	.136	.416	.454
.20	.000	.074	.074	.133	.222	.192	.187	.000	.380	.275	.295	.714
.23	.000	.063	.236	.205	.269	.461	.526	.263	.152	.404	.320	.066
.26	.000	.000	.000	.000	.250	.000	.199	.231	1.000	.538	.323	.000
.30	.166	.244	.166	.176	.380	.000	.375	.303	.399	.263	.386	.608
.40	.032	.234	.338	.441	.347	.239	.513	.408	.381	.479	.507	.578
	.068	.207	.239	.464	.361	.468	.388	.398	.690	.482	.555	.757
.06	.000	.046	.025	.026	.035	.071	.021	.027	.052	.052	.156	.333
.09	.034	.049	.062	.054	.019	.102	.017	.208	.000	.250	.076	.428
.12	.033	.079	.095	.103	.099	.113	.097	.152	.066	.187	.250	.413
.14	.024	.018	.111	.119	.058	.210	.204	.324	.428	.000	.500	.500
.16	.000	.107	.125	.159	.074	.101	.377	.256	.133	.000	.444	.333
.18	.000	.098	.130	.223	.112	.295	.170	.309	.090	.199	.321	.333
.20	.058	.114	.149	.203	.181	.241	.218	.121	.421	.250	.333	.428
.23	.047	.076	.181	.125	.263	.285	.235	.500	.199	.222	.176	.599
.26	.066	.000	.161	.136	.277	.238	.349	.230	.500	.363	.454	.687
.30	.272	.235	.187	.156	.399	.269	.275	.299	.352	.333	.444	.666
.40	.185	.382	.266	.254	.339	.295	.479	.361	.526	.399	.565	.424
	.375	.500	.333	.349	.307	.166	.705	.333	.799	.399	1.000	1.000

Table 2A. Radiosonde severe weather probabilities for given values from table 1. This table equivalent to middle row of Figure 2.

Class interval dividers (percentages)	Class interval divider (percentage)											
	.06	.09	.12	.14	.16	.18	.20	.23	.26	.30	.40
.06	.008	.014	.015	.015	.008	.043	.000	.095	.079	.030	.064	.086
.09	.033	.099	.056	.043	.066	.000	.039	.045	.000	.384	.148	.099
.12	.047	.041	.097	.096	.157	.181	.000	.103	.137	.351	.266	.208
.14	.042	.000	.062	.058	.153	.000	.199	.000	.083	.058	.473	.470
.16	.024	.129	.154	.205	.166	.083	.049	.086	.227	.214	.233	.529
.18	.000	.199	.071	.000	.000	.041	.199	.166	.000	.285	.357	.500
.20	.049	.222	.184	.166	.363	.500	.000	.143	.083	.000	.500	.500
.23	.000	.041	.207	.230	.214	.000	.500	.346	.375	.428	.157	.500
.26	.083	.258	.221	.349	.181	.000	.399	.343	.250	.277	.343	.466
.30	.187	.000	.272	.166	.272	.000	.143	.399	.428	.176	.406	.692
.40	.084	.115	.231	.288	.299	.333	.424	.399	.375	.476	.490	.666
	.217	.593	.444	.466	.433	.416	.530	.333	.509	.527	.613	.733

Table 3A. Radiosonde probability of severe weather for given values from Table 2. This table equivalent to last table in Figure 2 of text.

Showalter index degrees	850 mb wind speed--meters/second 4.5	7.5	11.0	14.5	18.5	23.0
-1.0	.269	.178	.217	.283	.383	.457	.426
2.0	.153	.118	.222	.319	.246	.276	.329
4.0	.041	.086	.147	.189	.273	.293	.239
6.0	.083	.060	.124	.177	.205	.337	.288
8.5	.062	.046	.077	.099	.092	.187	.093
12.0	.021	.041	.042	.058	.011	.051	.024
	.003	.010	.000	.000	.000	.000	.000

300 mb wind speed meters/second	shear term -80.	-40.	-1.0	1.0	60.0	100.0
13.0	.042	.065	.015	.076	.096	.158	.172
18.0	.021	.019	.045	.099	.180	.140	.106
23.0	.050	.021	.110	.237	.333	.140	.212
28.0	.071	.087	.074	.234	.443	.305	.278
34.0	.076	.078	.108	.162	.429	.313	.084
42.0	.055	.159	.131	.139	.268	.166	.119
	.117	.065	.213	.224	.172	.090	.000

850 mb temp.advect. degr./8 hours	500 mb wind speed--meters/second 8.0	11.0	15.0	20.0	25.0	30.0
-2.5	.169	.111	.058	.082	.054	.071	.023
-0.5	.049	.087	.102	.088	.111	.083	.097
0.0	.111	.056	.049	.154	.191	.157	.272
0.5	.117	.127	.104	.178	.228	.173	.174
1.5	.068	.128	.161	.147	.215	.210	.163
2.5	.085	.163	.175	.242	.238	.223	.276
	.111	.105	.129	.256	.321	.272	.192

Δ Showalter degr./8 hours	500 mb temp. advection--degr./8 hours -2.0	-1.0	-0.3	0.3	1.0	2.0
-10.	.180	.294	.206	.127	.203	.203	.226
-4.0	.024	.117	.138	.172	.212	.197	.296
-1.0	.000	.080	.099	.164	.165	.178	.189
1.0	.029	.063	.063	.121	.145	.136	.188
4.0	.125	.111	.119	.120	.130	.158	.146
7.0	.095	.000	.000	.142	.184	.114	.093
	.048	.133	.235	.210	.176	.259	.113

Table 4A. Satellite severe weather probabilities for given classes of predictors. This table equivalent to top row of Figure 2 in text.

class interval dividers (percentages)	.06	.09	.12	.14	.16	.18	.20	.23	.26	.30	.40
.06	.013	.019	.021	.008	.017	.083	.000	.038	.017	.000	.023	.034
.09	.005	.071	.084	.033	.157	.111	.199	.156	.018	.055	.090	1.000
.12	.018	.048	.139	.214	.074	.129	.000	.128	.032	.230	.304	.153
.14	.000	.032	.125	.000	.266	.166	.199	.166	.066	.333	.384	.000
.16	.036	.161	.044	.181	.220	.083	.166	.199	.297	.250	.125	.500
.18	.051	.079	.191	.000	.215	.119	.500	.473	.289	.500	.428	.272
.20	.000	.137	.264	.199	.103	.119	.500	.318	.176	.250	.294	.333
.23	.199	.205	.163	.151	.194	.177	.222	.416	.192	.177	.177	.416
.26	.000	.105	.068	.199	.205	.222	.333	.500	.384	.285	.500	.230
.30	.101	.152	.215	.272	.198	.199	.210	.396	.500	.593	.362	.407
.40	.192	.229	.186	.281	.242	.382	.428	.269	.547	.399	.464	.615
	.000	.250	.304	.363	.299	.511	.000	.125	.484	.333	.603	.738
.06	.000	.027	.038	.072	.070	.046	.029	.113	.166	.166	.166	.166
.09	.024	.068	.076	.094	.088	.076	.094	.145	.250	.000	.083	.124
.12	.029	.046	.071	.092	.068	.164	.199	.116	.199	.333	.208	.166
.14	.000	.166	.095	.097	.085	.160	.117	.054	.500	.399	.304	.235
.16	.037	.151	.105	.168	.176	.191	.111	.209	.354	.076	.190	.212
.18	.000	.171	.166	.180	.127	.165	.142	.216	.599	.368	.279	.246
.20	.000	.105	.153	.161	.242	.291	.132	.191	.500	.352	.316	.281
.23	.052	.076	.241	.243	.099	.245	.250	.281	.000	.411	.363	.322
.26	.000	.199	.225	.198	.306	.246	.236	.318	.000	.214	.289	.305
.30	.117	.000	.134	.206	.260	.437	.310	.279	.000	.351	.320	.313
.40	.117	.058	.333	.304	.599	.416	.217	.323	.000	.261	.291	.302
	.117	.088	.210	.257	.428	.422	.320	.321	.160	.211	.251	.276

Table 5A. Satellite severe weather probabilities for given values from Table 4. This table equivalent to middle row of figure 2 in text.

Class interval dividers (percentages)	.06	.09	.12	.14	.16	.18	.20	.23	.26	.30	.40
.06	.003	.018	.014	.000	.035	.020	.026	.053	.029	.037	.089	.000
.09	.000	.037	.075	.043	.041	.132	.083	.208	.049	.133	.133	.153
.12	.063	.035	.153	.000	.000	.196	.222	.294	.000	.000	.125	.000
.14	.071	.048	.108	.076	.000	.125	.192	.500	.173	.000	.363	.500
.16	.027	.095	.044	.000	.285	.271	.157	.250	.105	.166	.222	.000
.18	.074	.171	.064	.143	.111	.259	.107	.111	.062	.333	.307	.153
.20	.112	.172	.120	.187	.143	.250	.266	.219	.217	.285	.115	.583
.23	.080	.202	.302	.000	.250	.233	.244	.000	.285	.272	.222	.500
.26	.000	.272	.125	.000	.750	.125	.238	.214	.272	1.000	.466	.750
.30	.174	.290	.199	.545	.199	.271	.324	.368	.447	.000	.259	.299
.40	.189	.236	.212	.190	.333	.380	.366	.375	.479	.363	.530	.714
	.149	.232	.406	.500	.470	.604	.455	.480	.512	.603	.649	.866

Table 6A. Satellite probability of severe weather for given values from Table 5. This table equivalent to last row of Figure 2 in text.

NOAA SCIENTIFIC AND TECHNICAL PUBLICATIONS

The National Oceanic and Atmospheric Administration was established as part of the Department of Commerce on October 3, 1970. The mission responsibilities of NOAA are to assess the socioeconomic impact of natural and technological changes in the environment and to monitor and predict the state of the solid Earth, the oceans and their living resources, the atmosphere, and the space environment of the Earth.

The major components of NOAA regularly produce various types of scientific and technical information in the following kinds of publications:

PROFESSIONAL PAPERS—Important definitive research results, major techniques, and special investigations.

CONTRACT AND GRANT REPORTS—Reports prepared by contractors or grantees under NOAA sponsorship.

ATLAS—Presentation of analyzed data generally in the form of maps showing distribution of rainfall, chemical and physical conditions of oceans and atmosphere, distribution of fishes and marine mammals, ionospheric conditions, etc.

TECHNICAL SERVICE PUBLICATIONS—Reports containing data, observations, instructions, etc. A partial listing includes data serials; prediction and outlook periodicals; technical manuals, training papers, planning reports, and information serials; and miscellaneous technical publications.

TECHNICAL REPORTS—Journal quality with extensive details, mathematical developments, or data listings.

TECHNICAL MEMORANDUMS—Reports of preliminary, partial, or negative research or technology results, interim instructions, and the like.

Information on availability of NOAA publications can be obtained from:

PUBLICATION SERVICES BRANCH (E/AI13)
NATIONAL ENVIRONMENTAL SATELLITE, DATA, AND INFORMATION SERVICE
NATIONAL OCEANIC AND ATMOSPHERIC ADMINISTRATION
U.S. DEPARTMENT OF COMMERCE

Washington, DC 20235

NOAA--S/T 83-136